Astron. Astrophys. 323, 529–533 (1997)

ASTRONOMY AND ASTROPHYSICS

*Research Note*

# Intense molecular emission from the Lagoon nebula, M8

**Glenn J. White**[1], **N.F.H. Tothill**[1], **H.E. Matthews**[2], **W.H. McCutcheon**[3], **M. Huldtgren**[4], **and Mark J. McCaughrean**[5,6]

[1] Department of Physics, Queen Mary & Westfield College, University of London, Mile End Road, London E1 4NS, UK
[2] Joint Astronomy Centre, 660 N A'ōhōku Place, University Park, Hilo, Hawaii 96720, USA
[3] Department of Physics and Astronomy, University of British Columbia, Vancouver, British Columbia V6T 1Z1, Canada
[4] Stockholm Observatory, S-133 36 Saltsjöbaden, Sweden
[5] Max-Planck-Institut für Astronomie, Königstuhl, D-69117 Heidelberg, Germany
[6] Max-Planck-Institut für Radioastronomie, Auf dem Hügel 69, D-53121 Bonn, Germany

Received 21 January 1997 / Accepted 21 March 1997

**Abstract.** The discovery is reported of the second strongest source of mm and submm wavelength CO line emission, towards M8, the Lagoon Nebula in Sagittarius. The $\sim$31 $M_\odot$ molecular core has dimensions $\sim 0.2 \times 0.3$ pc and is centred on the O7V star Herschel 36 (H 36), near the Hourglass Nebula in the core of M8. Emission from the CO line wings extends to the north and south of the Hourglass, although a lack of near-IR $H_2$ emission indicates that outflow activity is much less prominent than in many active star-formation regions, and suggests that the CO line wings may trace the expanding edge of a cavity around H 36. The molecular line data are compared with new near-IR narrow-band, continuum-subtracted images in He I, $H_2$, and $H^+$ (Br$\gamma$) lines and archival HST emission-line images in H$\alpha$, [O III], and [S II]. The optical and near-IR data are found to be broadly consistent with previous photo-ionisation models of the Hourglass, which is excited by H 36. However, there are variations in the He I/Br$\gamma$ line ratio which are difficult to explain.

**Key words:** ISM: individual objects: M8– ISM: molecules – radio lines: ISM

## 1. Introduction

M8, the Lagoon Nebula (NGC 6523), is one of the most prominent H II regions in the Galaxy. It has been studied over a wide range of wavelengths, as summarised by Lada et al. (1976), Elliot et al. (1984), Woodward et al. (1986) and Stecklum et al. (1995). The excitation conditions in the central region of M8 are dominated by the radiation from recently formed OB stars interacting strongly with the surrounding gas, especially the O7V star H 36, which excites the well-known Hourglass Nebula. In this paper, new molecular line maps and narrow-band near-IR images of the H 36 region are reported, and compared with a broad-band 2$\mu$m image and archival HST emission-line images.

*Send offprint requests to*: Prof Glenn White

## 2. The Observations

Observations of CO and isotopomeric $J = 2-1$, $J = 3-2$, $J = 4-3$ rotational transitions, and the $^3P_1 - {}^3P_0$ atomic carbon fine structure line were made with standard facility receivers on the 15 metre James Clerk Maxwell Telescope (JCMT) in Hawaii. Maps in the various lines were made on grids at half beamwidth spacings, with spectral velocity resolutions $\sim$ 0.3 km s$^{-1}$, and were calibrated in units of corrected antenna temperature $T_r^*$ (=$T_a^*/\eta_{fss}$). The absolute calibration uncertainties at the frequencies of the CO lines were $J = 2-1 : \leq 12$ %, $J = 3-2 : \leq 14\%$ and $J = 4-3 : \leq 20\%$. The calibration scale was confirmed by observing JCMT spectral line calibration standards, whose intensities appeared nominal. Details of the observations are listed in Table 1. At the distance of M8 (1.5 kpc - Georgelin and Georgelin 1976), 10″ corresponds to a linear size of 0.07 pc.

Near-IR narrow-band ($\Delta\lambda/\lambda \sim 1\%$) observations of the He I $2^1P$–$2^1S$ ($\lambda$2.058$\mu$m), $H_2$ v=1–0 S(1) ($\lambda$2.122$\mu$m), and $H^+$ Br$\gamma$ ($\lambda$2.166$\mu$m) lines were made during July 1996 using IRAC-2 at the ESO/MPG 2.2 metre telescope on La Silla. The camera was used in its 0.5″ /pixel mode, covering a $2 \times 2'$ field of view; the seeing during these observations was 1.5″ FWHM. In each filter, five dithered 30 second exposures were made and mosaiced together. The absolute calibration accuracy of the narrow-band images is $\sim$0.5 magnitudes RMS. A broad-band K′ frame taken using IRIS on the 3.9 m Anglo-Australian Telescope (with 0.8″ /pixel and 2″ FWHM seeing) was used to

**Table 1.** JCMT telescope parameters - April 1996

| Line | Transition | Freq GHz | HPBW | $\eta_{\rm mb}$ | $\eta_{\rm fss}$ |
|---|---|---|---|---|---|
| $C^{18}O$ | $J = 2-1$ | 219.560 | $22''$ | 0.69 | 0.80 |
| $^{13}CO$ | $J = 2-1$ | 220.398 | $21''$ | 0.69 | 0.80 |
| CO | $J = 2-1$ | 230.538 | $19''$ | 0.69 | 0.80 |
| $C^{18}O$ | $J = 3-2$ | 329.331 | $15''$ | 0.58 | 0.70 |
| $^{13}CO$ | $J = 3-2$ | 330.588 | $15''$ | 0.58 | 0.70 |
| CO | $J = 3-2$ | 345.796 | $14''$ | 0.58 | 0.70 |
| CO | $J = 4-3$ | 461.041 | $11''$ | 0.53 | 0.70 |
| C I | $^3P_1 - ^3P_0$ | 492.160 | $10''$ | 0.49 | 0.67 |

assess the continuum emission in the line filters. The emission-line images were smoothed to the same point spread function as the continuum image; aperture photometry was then used to measure stellar fluxes in both; finally, the continuum image was scaled and subtracted from the narrow-band images.

## 3. Molecular and CI line data

The CO lines at the position of H 36 are unusually intense, with peak $T_{\rm r}^*$ values $\sim$ 100 K, corresponding to main beam brightness temperatures (see Table 1), $T_{\rm mb}$ = 115 K (CO $J = 2-1$), 120 K (CO $J = 3-2$) 125 K (CO $J = 4-3$), 33 K ($^{13}$CO $J = 2-1$), 40 K ($^{13}$CO $J = 3-2$), 6.8 K ($C^{18}O$ $J = 2-1$) and 9.2 K ($C^{18}O$ $J = 3-2$). Several CO $J = 3-2$ spectra are shown in Fig. 1. **This is the second most intense CO source observed with a single dish antenna; it is remarkable that it has remained unreported for so long.**

The region centred on H 36 was mapped in various lines, as shown in Fig. 2 (see next page). Inspection of parts of the spectra away from the lines reported in this paper suggests that the source does not contain the large numbers of strong lines seen, for example, towards the Orion Hot Core.

The integrated CO $J = 3-2$ emission peaks at H 36 (peak velocity 10.0 km s$^{-1}$), and $\sim 40''$ to the NW (10.7 km s$^{-1}$). A faint extension to the CO emission extending from H 36 to the SW at 11.2 km s$^{-1}$, is associated with a region of extinction seen in Fig. 2j–l. Four peaks can be identified in the higher angular resolution CO $J = 4-3$ map; the most intense at (−9,10) lies close to the IR sources detected by Woodward et al. (1986); the second most intense peak centred $6''$ W of H 36 – extends $\sim 10''$ eastward towards the B4 V star KS2 (Woodward et al. 1990); the third peak at (+29, −2) lies close to an 11 $\mu$m source IRS2 (Dyck 1977), and the fourth at (−32, −31) traces the previously mentioned foreground extinction.

The velocity structure close to H 36 can be seen in the $^{13}$CO $J = 3-2$ map in Fig. 3. Between 7 and 9 km s$^{-1}$, the emission comes from the NW of H 36, and from 8.5 and 11 km s$^{-1}$ the emission peaks $\sim 10''$ E and W of H 36, straddling the position of the star (see the 10.25 km s$^{-1}$ channel). Emission from this central region then divides into further peaks $\sim 20''$ NW of H 36 in the 10.75 km s$^{-1}$ map. A less intense peak is also seen at

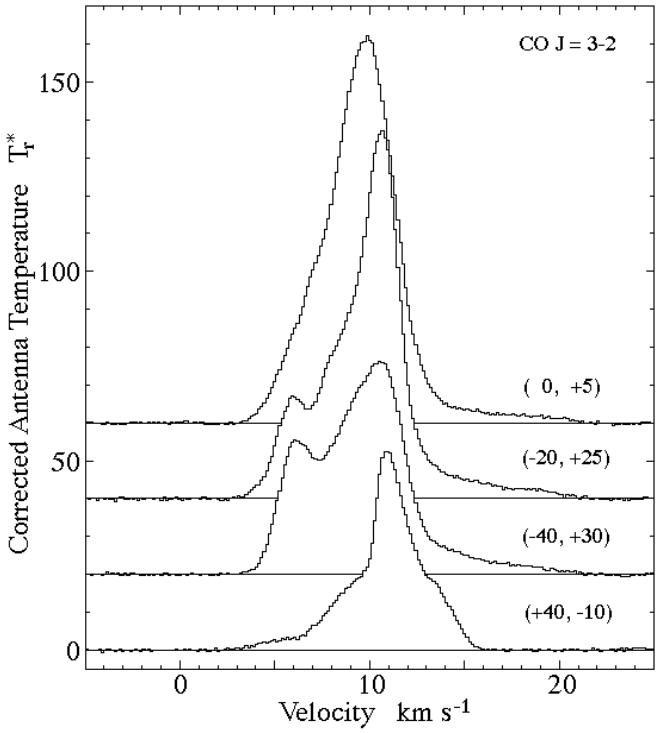


**Fig. 1.** CO spectra close to H 36 (offsets shown in arcseconds). The (0,0) position for this and the maps is that of H 36: $\alpha_{1950} = 18^h\ 00^m\ 36.3^s$, $\delta_{1950}$ = -24°22′ 53″ . By comparison, the peak CO $J = 3-2$ line intensity of the most intense known source, Orion A, is $\sim$ 130 K, under similar calibration conditions.

(−20,−40), at $\sim$ 11.25 km s$^{-1}$, where the optical obscuration is seen on the HST images.

As shown in Fig. 1, emission in the CO line wings extends over a range of $\sim$ 20 km s$^{-1}$. The spatial distribution of the wings is complex; the red-shifted gas lies predominantly to the north, and blue-shifted gas dominates close to H 36 and the Hourglass Nebula. Emission in high velocity line wings is often interpreted as being a tracer of outflowing gas, but the lack of $H_2$ emission (see later) may suggest instead that some of the predominantly blue-shifted wing emission traces material at the edge of the cavity surrounding H 36. However, we cannot rule out an outflow interpretation at this stage, particularly in view of the near-IR jet reported by Stecklum et al. (1995).

The integrated $C^{18}O$ $J = 3-2$ map peaks at (5,5), close to KS2, and has a size of $\sim 30\times20''$, oriented SE-NW. The peak column density N($C^{18}O$) is 2.1 $10^{16}$ cm$^{-2}$, or N($H_2$) = 1.3 $10^{23}$ cm$^{-2}$ (for [$C^{18}O$]/[$H_2$] = 1.6 $10^{-7}$). As an independent estimate, an LVG code was used to simultaneously fit the intensities of the CO and isotopomeric data listed earlier, gave a best estimate of $n(H_2)$= 7 $10^3$ cm$^{-3}$ and $N_{\rm col}$ /dv/dr = 2 $10^{18}$ cm$^{-2}$ km$^{-1}$ s pc. From the $C^{18}O$ $J = 3-2$ map, we estimate dv/dr $\gtrsim$ 14 km s$^{-1}$ pc$^{-1}$, so the LVG upper limit for N($C^{18}O$) = 6 $10^{16}$ cm$^{-2}$. Assuming the core has similar dimensions along the line of sight to that seen in the plane of the sky, and that it has a constant volume density, its mass is $\sim$ 31 $M_\odot$.

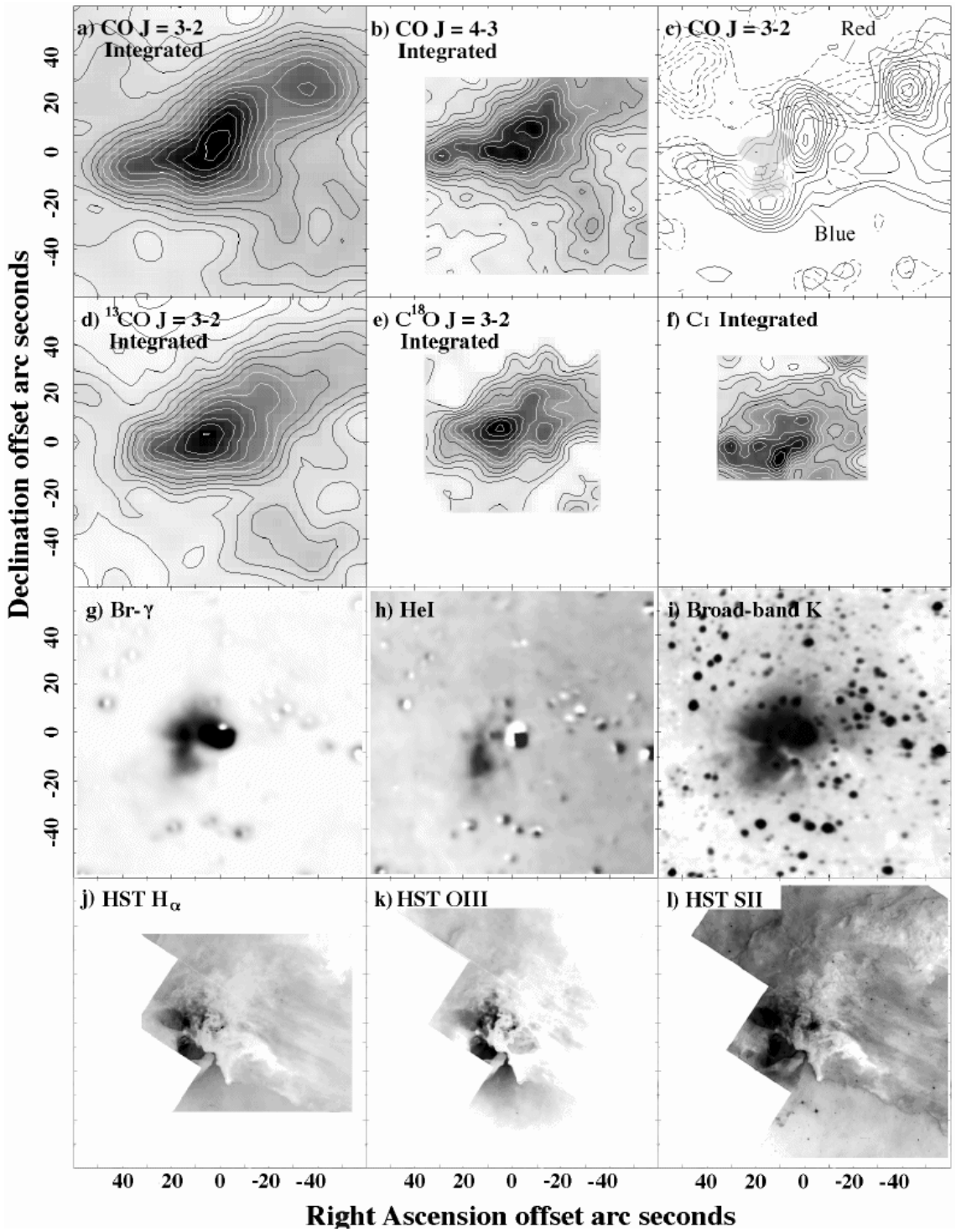


**Fig. 2a–l.** Maps and images of the Hourglass region. The exciting source H 36 is located at 0,0 in each frame. **a** integrated CO $J = 3 - 2$ emission ($2 - 23$ km s$^{-1}$). **b** integrated CO $J = 4 - 3$ . **c** high velocity blue (0 - 5.5 km s$^{-1}$) and red (15 - 20.5 km s$^{-1}$) emission, with the Hourglass Nebula indicated by the shaded region close to the centre. **d** $^{13}$CO $J = 3 - 2$ integrated emission. **e** C$^{18}$O $J = 3 - 2$ integrated emission. **f** CI integrated emission. **g** continuum-subtracted Br$\gamma$ , *the residual stellar images in this and Fig. 2*. **h** *result from imperfect continuum subtraction, and are at the level of about 1% of the peak flux of H 36*. **h** continuum-subtracted He I. **i** broad-band AAT K′ (used as the continuum to prepare **g** and **h**). **j** HST Archive H$\alpha$ . **k** HST Archive [O III]. **l** HST [S II]. The first white contour and the steps are respectively **a** (230, 30 K km s$^{-1}$), **b** (225, 25 K km s$^{-1}$), **c** (blue: lowest contour at 5 K km s$^{-1}$, steps at 5 K km s$^{-1}$, red: lowest contour at 2.5 K km s$^{-1}$, steps at 2.5 K km s$^{-1}$), **d** (90, 10 K km s$^{-1}$), **e** (14, 2 K km s$^{-1}$), **f** (25, 2.5 K km s$^{-1}$). The near-IR and optical images are shown with logarithmic scaling, except **g** and **h** which have linear scales.

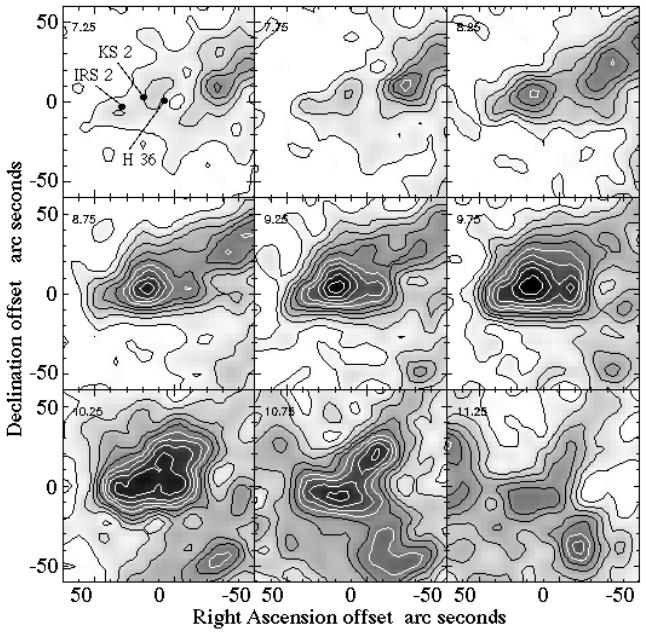


**Fig. 3.** Channel maps of the $^{13}$CO $J = 3 - 2$ emission in 0.5 km s$^{-1}$ channel widths. The (0,0) position is $\alpha_{1950}$ = $18^h\ 00^m\ 36.3^s$, $\delta_{1950}$ = -24°22′ 53″ , and the first white contour is at 11 K km s$^{-1}$ and the interval is 2 K km s$^{-1}$ . The positions of several infrared sources discussed in this paper are indicated with filled circles.

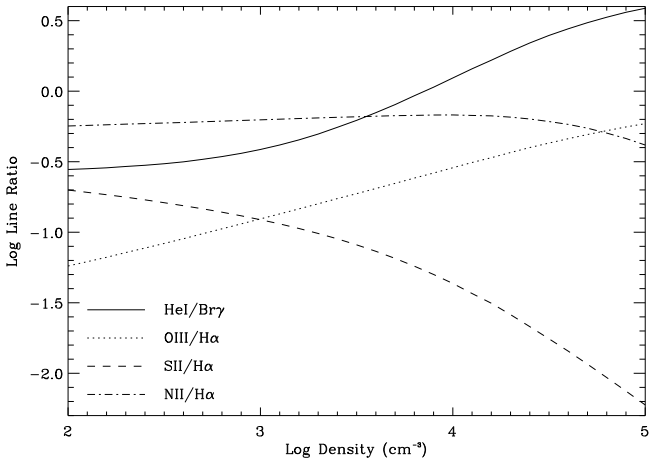


**Fig. 4.** Ratios of line intensities calculated using CLOUDY 90.02 as described in the text

The integrated CI emission peaks at (+10, -6), just south of H 36 (where it has a value of 42 K km s$^{-1}$ ), and at (30, -3) (39 K km s$^{-1}$ ), close to the third most intense CO peak and the 11 $\mu$m source reported by Dyck (1977). There is no prominent emission at H 36 or at the intense CO peak to its north. This follows the trend noted previously by White & Padman (1991) and White & Sandell (1995) for CI and CO peaks to be offset from each other, which can be understood if the CI traces warm surface layers of dense neutral clumps. Assuming that $T_{\rm ex}$ (CI) $\sim$ $T_{\rm ex}$ (CO), the column density at H 36, N(CI) = 7 $10^{17}$ cm$^{-2}$ , and the abundance ratio [CI]/[CO] = 0.07, typical of ratios found in dense molecular cloud cores (White & Sandell 1995).

## 4. Infrared and optical data

The continuum-subtracted $H_2$ image showed no evidence for diffuse line emission from the Hourglass region to $\leq$ 3.4 $10^{-4}$ erg s$^{-1}$ cm$^{-2}$ sr$^{-1}$. The corresponding $H_2$ column density upper limit is 9.9 $10^{17}$ cm$^{-2}$ (following Gautier et al. 1976, Brand et al. 1988); more than 20 times less than the $H_2$ seen reported towards Peak 1 in the Orion Nebula (Beckwith et al. 1978).

The relative intensities of the He I and Br$\gamma$ lines vary by a factor of $\sim$ 3 across the Hourglass Nebula: He I emission is prominent in the southern lobe, while Br$\gamma$ emission is stronger in the northern lobe and near H 36. In a classical Strömgren sphere this ratio should remain constant, except near the edge of the HII region. The observed variation cannot be a consequence of extinction; a change in the intensity ratio of only 20 % would require $A_v \sim$ 20 magnitudes, whereas Woodward et al. (1986) estimate that $A_v$ is only $\sim$ a few magnitudes at most towards the optically-visible Hourglass.

The variation in the He I/Br$\gamma$ ratio is more likely to be due to changes in excitation than extinction. The He I line is enhanced by collisional depopulation at a critical density $\sim$ $10^3$ cm$^{-3}$ (Doyon et al. 1992), similar to that of the Hourglass region (4.4 $10^3$ cm$^{-3}$ ). It therefore seems plausible that the HeI/Br$\gamma$ ratio variation could result from density variations within the HII region. To test this, the photoionisation code Cloudy 90.02 (Ferland 1996) was used to calculate the emitted intensity ratios of various lines from a spherical HII region illuminated by a 35,000 K star (*i.e.*, the O7V H 36) with a Kurucz model atmosphere, as a function of hydrogen density, $n_{H_2}$, as shown in Fig. 4.

The He I/Br$\gamma$ intensity ratio varies markedly over the range of densities of interest: but $n_{H_2}$ would need to change by a factor of $\sim$10 to reproduce the observed line ratio change. This same density variation would also predict changes in the ratios of [O III]/H$\alpha$ and [S II]/H$\alpha$ of factors of 2 and 3–4 respectively, changes which are not found in the HST data.

Woodward et al. (1986) published radio observations of M8; at 5 GHz where the nebula is optically thin, the flux density $S_\nu$ $\propto n_e^2$. From their radio map there is no brightness enhancement apparent in the southern part of the Hourglass; hence the density cannot differ much from the average. It is therefore unlikely that the change in the He I/Br$\gamma$ ratio is a consequence of electron density contrasts in the H II region. Other mechanisms must be sought to explain how this ratio varies. Possible explanations are abundance effects and the role of dust in the radiative transfer processes in the H II region. Further simulations suggest that the change of line intensity with abundance is roughly linear over the density range of interest; an enhancement of He I by $\sim$ 3 would require at least a doubling of the He abundance, which is difficult to argue for without further observational evidence.

## 5. Conclusions

The detection of the second strongest source of mm and submm CO line emission is reported towards the Lagoon Nebula, M8. A molecular core with a size $\sim 0.2\times0.3$ pc and mass $\sim 31$ $M_\odot$ is centred close to the O7 star Herschel 36. The lack of near-IR $H_2$ emission suggests that shock activity is very weak, and we speculate that CO line wings may instead trace the expanding edge of the cavity around H 36. Near-IR narrow-band continuum-subtracted images in He I, $H_2$, and Br$\gamma$ lines were compared with the molecular line data and HST narrow band H$\alpha$ , [O III], and [S II] images. Although they are broadly consistent with predictions of the Woodward et al. (1986) model, the variability of the HeI/Br$\gamma$ ratio is unexplained. Comparison with HST and radio observations suggest this is not related to density or abundance variations.

*Acknowledgements.* We thank the JCMT and ESO TO's and support scientists for their help; Prof S Beckwith for allocating MPG observing time on the ESO/MPG 2.2m; PPARC for travel funds; Prof Gary Ferland for providing the CLOUDY code for the community-at-large. The K′ frame was archival data from the Anglo Australian Telescope, taken by Dr David Allen, and kindly made available by Dr David Malin. The JCMT is operated by the JAC on behalf of PPARC, NWO and the NRC. The HST data were based on operations made with the NASA/ESA Hubble Space Telescope, obtained from the data archive at the Space Telescope Science Institute. STScI is operated by the Association of Universities for Research in Astronomy, Inc., under NASA contract NAS5-26555.

## References

Beckwith, S., Persson, S.E., Neugebauer, G., Becklin, E.E. 1978, ApJ 223, 464.
Brand, P.W.J.L., Moorhouse, A., Burton, M.G., Geballe, T.R., Bird, M., Wade, R. 1988, ApJ 334, L103.
Doyon, R., Puxley, P.J., Joseph, R.D. 1992, ApJ 397, 117.
Dyck, H.M. 1977, AJ 82, 129.
Elliot, K.H., Goudis, C., Hippelein., H. Meaburn, J. 1984, A&A 138, 451.
Ferland, G.J. 1996, University of Kentucky, Department of Physics and Astronomy Internal Report.
Gautier, T.N., Fink, U., Treffers, R.R. Larson, H.P. 1976, ApJ 207, L129.
Georgelin, Y.M., Georgelin, Y.P. 1976, A&A 49, 57.
Lada, C.J., Gull, T.R., Gottlieb, C.A., Gottlieb, E.W. 1976, ApJ 203, 159
Stecklum, B., Henning, T., Eckart, A., Howell, R.R., Hoare, M.G. 1995, ApJ, 445, L153
White, G.J., Padman, R. 1991, Nature 354, 511
White, G.J., Sandell, G. 1995 A&A, 299, 179.
Woodward, C.E., Pipher, J.L., Helfer, H.L., Sharpless, S., Moneti, A., Kozikwski, D., Oliveri, M., Willner, S.P., Lacasse, M.G., Herter, T. 1986, AJ 91, 870
Woodward, C.E., Pipher, J.L., Helfer, H.L., Forrest, W.J. 1990, ApJ 365, 252

This article was processed by the author using Springer-Verlag LaTeX A&A style file *L-AA* version 3.